

# Astigmatism-corrected miniature Czerny-Turner spectrometer with freeform cylindrical lens

Guo Xia (夏 果), Bixiang Qu (屈碧香), Peng Liu (刘 鹏), and Feihong Yu (余飞鸿)\*

Optical Engineering Department, Zhejiang University, Hangzhou 310027, China

\*Corresponding author: feihong@zju.edu.cn

Received December 9, 2011; accepted March 29, 2012; posted online June 15, 2012

A miniature, broadband, astigmatism-corrected Czerny-Turner spectrometer is proposed. Theories of the broadband astigmatism correction using freeform cylindrical lens are thoroughly analyzed. Comparisons of the freeform cylindrical lens method with those of titling cylindrical lens or wedge cylindrical lens methods are also described. Results show the better spectrometer performance with the new optical design over a broadband spectral range from 300 to 800 nm.

OCIS codes: 120.6200, 120.4570, 300.6190.

doi: 10.3788/COL201210.081201.

The Czerny-Turner spectrometer, which includes a plane grating and two spherical mirrors, is an optical instrument used to measure light spectral properties. Several applications, such as spatially resolved ultrashort pulse measurement<sup>[1]</sup>, atmospheric sounding<sup>[2]</sup>, frequency-domain optical coherence tomography<sup>[3,4]</sup>, and femtosecond pulse characterization<sup>[5]</sup>, require high-quality imaging along the one-dimensional detector simultaneity. However, in the traditional Czerny-Turner spectrometer, the off-axis reflects light<sup>[6]</sup> from the spherical imaging mirror, including astigmatism, due to the different focal lengths in tangential and sagittal planes.

Some potential methods of reducing or removing astigmatism have been investigated, such as the spherical or toroidal focusing mirror method<sup>[7]</sup>, compensating optics before the entrance slit<sup>[8]</sup>, adding a convex mirror<sup>[9]</sup>, cylindrical grating<sup>[10]</sup>, or using freeform mirrors<sup>[11]</sup>. However, these methods may limit the spectrometer design for other specifications.

Recent spectrometer designs include introducing divergent illumination<sup>[12]</sup>, tilting a cylindrical lens<sup>[13]</sup>, and using a wedge cylindrical lens<sup>[14]</sup>. Divergent illumination eliminates the astigmatism; however, it induces coma, which influences imaging quality. With tilting or wedge cylindrical lens, astigmatism cannot be completely corrected for miniature fiber spectrometer with a broadband spectral range from 300 to 800 nm.

In this letter, we design a miniature Czerny-Turner spectrometer with a freeform cylindrical lens located close to the detector<sup>[15]</sup>. With our design, astigmatism can be corrected over a broadband spectrum. Theories of the broadband astigmatism compensation using a freeform cylindrical lens are thoroughly analyzed. Comparisons of the freeform cylindrical lens method with those of titling cylindrical lens or wedge cylindrical lens methods are described.

The difference in astigmatic foci  $\Gamma_a$  generated by two off-axis spherical mirrors of a Czerny-Turner spectrometer can be derived as<sup>[9]</sup>

$$\Gamma_a = (R_1/2)(\sin \alpha_1 \tan \alpha_1) + (R_2/2)(\sin \alpha_2 \tan \alpha_2), \quad (1)$$

where  $R_1$  is the radius of the first spherical mirror,  $R_2$  is the radius of the second spherical mirror,  $\alpha_1$  is the off-

axis ray incident angle on the first mirror, and  $\alpha_2$  is the off-axis ray incident angle on the second mirror.

In this design, a freeform cylindrical lens is located close to the detector, as shown in Figs. 1(a) (sagittal view) and (b) (tangential view).

The difference of the sagittal object focus of cylindrical lens  $s_{cs}$  and the central thickness of the cylindrical lens  $t_0$  is  $s_{cs} - t_0$ , as shown in Fig. 1(a). The sagittal lens equation of cylindrical lens is given as

$$\frac{n}{t_0} = \frac{1}{f_{cs}} + \frac{1}{s_{cs}}, \quad (2)$$

which yields

$$s_{cs} - t_0 = s_{cs} - \frac{f_{cs}s_{cs}}{f_{cs} + s_{cs}}n, \quad (3)$$

where the subscript  $c$  stands for cylindrical lens and  $f_{cs}$  is the sagittal focal length of the cylindrical lens.

The difference of  $t_0$  and the tangential focus of cylindrical lens  $s_{ct}$  is  $t_0 - s_{ct}$ , as shown in Fig. 1(b), which is given by

$$t_0 - s_{ct} = [(n-1)/n]t_0, \quad (4)$$

where  $n$  is the refractive index.

The astigmatism is removed when

$$\Gamma_a = s_{cs} - s_{ct} = s_{cs} - t_0 + t_0 - s_{ct}. \quad (5)$$

In the sagittal view, substituting Eqs. (3) and (4) into Eq. (5) gives

$$s_{cs}^2 - \Gamma_a s_{cs} - \Gamma_a f_{cs} = 0, \quad (6)$$

and  $s_{cs}$  can be derived as

$$s_{cs} = \frac{\Gamma_a + \sqrt{\Gamma_a^2 + 4\Gamma_a f_{cs}}}{2}, \quad (7)$$

where  $f_{cs} = \frac{R}{n-1}$ . Here,  $R$  is the radius of cylindrical lens at the central wavelength.

The incident angle of the focusing mirror varies with the different diffracted wavelengths with the different grating diffraction angles. The variation in  $\alpha$  across the

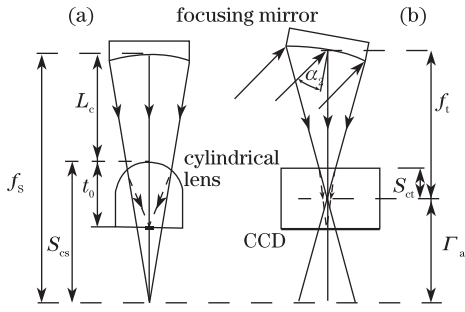


Fig. 1. Astigmatism correction by a cylindrical lens in (a) tangential view and (b) sagittal view on the detector. The solid rays denote the rays without the cylindrical lens, whereas the dashed rays denote the rays with the cylindrical lens.

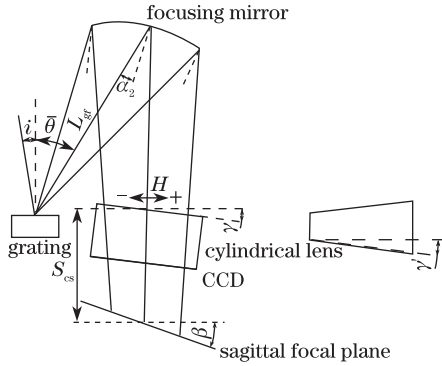


Fig. 2. Astigmatism correction by a freeform cylindrical lens in the tangential view for different wavelengths. Here,  $i$  is the angle incident on the grating.

focusing mirror results in a variation in astigmatism  $\Gamma_a$  along the image plane. As shown in Fig. 2, the incident angle of the ray of central wavelength is  $\alpha_2$ ,  $\beta$  is the tilt angle of the sagittal focal plane according to the chief ray, and  $\gamma$  is the tilt angle of the cylindrical lens. Here,  $H$  is the distance from the chief ray of the considered wavelength to the chief ray of the central wavelength. Astigmatism with the wavelength can be simultaneously compensated by the freeform cylindrical lens, which, according to Eqs. (3) and (4), Eq. (5) can be expressed as

$$\Gamma_a = s_{cs} - \frac{1}{n} \cdot t_0. \quad (8)$$

By differentiating Eq. (8) with respect to  $\lambda$ , one can obtain

$$\frac{d(\Gamma_a)}{d\lambda} = \frac{d(\Gamma_a)}{d\alpha_2} \cdot \frac{d\alpha_2}{d\theta} \cdot \frac{d\theta}{d\lambda} = \frac{ds_{cs}}{dH} \cdot \frac{dH}{d\lambda} + \frac{t_0}{n^2} \cdot \frac{dn}{d\lambda}, \quad (9)$$

where the first differentiation  $\frac{ds_{cs}}{dH}$  on the right side is derived from geometry in Fig. 2 as

$$\left. \frac{ds_{cs}}{dH} \right|_{H=0} = \tan(\beta + \gamma). \quad (10)$$

The second differentiation  $\frac{dH}{d\lambda}$  is the linear dispersion of the grating with respect to the wavelength of the light beam, which can be expressed as

$$\left. \frac{dH}{d\lambda} \right|_{\lambda=\lambda_c} = \frac{R_2}{2d \cos \bar{\theta}}, \quad (11)$$

where  $\lambda_c$  is the central wavelength and  $d$  is the grating period.

The first differentiation  $\frac{d(\Gamma_a)}{d\alpha}$  on the left side of Eq. (9) is calculated from Eq. (1), which can be expressed as

$$\left. \frac{d(\Gamma_a)}{d\alpha} \right|_{\alpha=\alpha_2} = (R_2/2) \sin \alpha_2 (1 + \sec^2 \alpha_2). \quad (12)$$

The second differentiation  $\frac{d\alpha}{d\theta}$  is derived from geometry as

$$\left. \frac{d\alpha}{d\theta} \right|_{\theta=\bar{\theta}} = 1 - (L_{gf}/R_2 \cos \alpha_2), \quad (13)$$

where  $L_{gf}$  is the distance between the grating and the focusing mirror. The third differentiation  $\frac{d\theta}{d\lambda}$  is the angular dispersion of the grating with the diffraction angle at the central wavelength:

$$\left. \frac{d\theta}{d\lambda} \right|_{\lambda=\lambda_c} = 1/d \cos \bar{\theta}. \quad (14)$$

Substituting Eqs. (10)–(14) into Eq. (9) gives

$$\begin{aligned} & \tan(\beta + \gamma) \frac{R_2}{2d \cos \bar{\theta}} + \frac{t_0}{n} \\ &= [(R_2/2) \sin \alpha_2 (1 + \sec^2 \alpha_2)] \\ & \cdot [1 - (L_{gf}/R_2 \cos \alpha_2)] [1/d \cos \bar{\theta}]. \end{aligned} \quad (15)$$

The tilt angle  $\gamma$  can be derived from Eq. (15).

By differentiating Eq. (5) with respect to  $\lambda$ , we obtain

$$\begin{aligned} \frac{d(\Gamma_a)}{d\lambda} &= \frac{d}{d\lambda} \left( s_{cs} - \frac{f_{cs} s_{cs}}{f_{cs} + s_{cs}} \right) = \frac{2s_{cs}(f_{cs} + s_{cs}) - s_{cs}^2}{(f_{cs} + s_{cs})^2} \\ & \cdot \frac{ds_{cs}}{dH} \cdot \frac{dH}{d\lambda} - \frac{s_{cs}^2}{(f_{cs} + s_{cs})^2} \cdot \frac{df_{cs}}{dR} \cdot \frac{dR}{dH} \cdot \frac{dH}{d\lambda}, \end{aligned} \quad (16)$$

where the differentiation  $\frac{df_{cs}}{dR}$  can be expressed as

$$\frac{df_{cs}}{dR} = \frac{1}{n-1}. \quad (17)$$

As shown in Fig. 3, the freeform cylindrical lens converges rays only in the  $y$  direction, whereas, in the  $x$  direction, it performs as a parallel plate. Therefore, deriving the surface function of cylindrical lens is simple, as shown in

$$z = \frac{cy^2}{1 + \sqrt{1 - (1+k)c^2y^2}}, \quad (18)$$

where  $c = \frac{1}{R}$ . For traditional cylindrical lens, the radius  $R$  along the  $x$  direction is constant, whereas, for freeform cylindrical lens,  $R$  varies with  $x$  coordinates, as related to the wavelength

$$R = a + bx, \quad (19)$$

where  $a$  and  $b$  are constants. Therefore, we define

$$\frac{dR}{dx} = \frac{dR}{dH} = \tan \gamma', \quad (20)$$

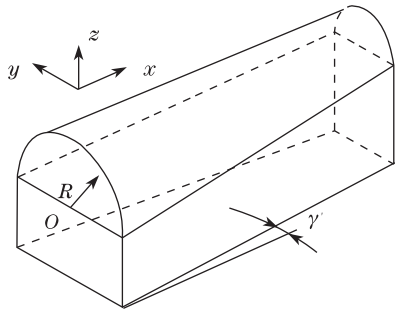


Fig. 3. Layout of the freeform cylindrical lens.

where  $\gamma'$  is the angle formed by the linear change of the radius of cylindrical lens, which can be solved from Eq. (16).

We present the design procedure for the broadband astigmatism-corrected miniature Czerny-Turner spectrometer. Firstly, for the spectrometer without cylindrical lens, the radii  $R_1$  and  $R_2$  of the two mirrors and the incident angles  $\alpha_1$  and  $\alpha_2$  are determined according to the slit, numerical aperture (NA, half width at  $1/e^2$ ), grating resolution, detector array size, and pixel number. Secondly, according to the derived astigmatism from Eq. (1), the radius  $R$  of the cylindrical lens at the central wavelength is determined according to the detector size. The sagittal object distance  $S_{cs}$  from Eq. (7), and the central thickness from Eq. (8) are also determined. Thirdly, the distance  $L_{gf}$ , tilt angle of the sagittal focal plane  $\beta$ , and tilt angle of the cylindrical lens  $\gamma$  are obtained. Finally, the angle  $\gamma'$  is derived according to Eq. (16). Thus, all the system parameters can be obtained and calculated. We programmed the derivation procedure in MATLAB, after which we optimized the system parameters using ray-tracing software CODE V. The spectrometer parameters are shown in Table 1. The initial and optimized parameters are shown in Table 2.

The astigmatism  $L_a$  at central wavelength (550 nm) was derived as 14.5157 mm using Eq. (1). The distance  $L_{fc}$ , which is related to the position of the cylindrical lens, was calculated as 52.9585 mm using Eqs. (6) and (7). This value is close to the optimized value (i.e., 52.97 mm). The tilt angle  $\gamma$  of the cylindrical lens was calculated to be  $26.5967^\circ$ , which is close to the optimized value (i.e.,  $25.853^\circ$ ). The angle  $\gamma'$  of the freeform cylindrical lens was calculated to be  $1.467^\circ$ , which is close to the optimized value (i.e.,  $2.24^\circ$ ). When the radius  $R$  of the cylindrical lens at the central wavelength was 2.75 mm, the central thickness  $t_0$  was derived as 6.30 mm; both values are close to the optimized values (i.e., 3.389 and 6.50 mm, respectively).

The design of miniature spectrometer using the parameters in Tables 1 and 2 is realized. The miniature fiber spectrometer is an UV-to-visible system with a spectral range from 300 to 800 nm and entrance slit size of  $1.2 \times 0.02$  (mm). The numerical aperture of the fiber is 0.05, and the fixed plane grating is 600 lp/mm. The cylindrical lens material is BK7, and its refractive index  $n$  is 1.5132 at the central wavelength of 550 nm. The charge-coupled device (CCD) sensor size is  $29.1 \times 0.2$  (mm) (pixel size is  $8 \times 200$  ( $\mu\text{m}$ ) and pixel number is 3648). Using CODE V, the optimized layout is shown in Fig. 4.

To verify the optical performance of the spectrometer, root mean square (RMS) spot size by ray tracing along the detector surface and the line spread function (LSF) at the central wavelength were calculated with both the new and the traditional systems.

As shown in Fig. 5(a), for the traditional system, the astigmatism is represented as a long and narrow shape in the spot diagram. For the new astigmatism-corrected system, the spot diagram is greatly compressed, as shown in Fig. 5(b).

The LSF is shown as a dotted line in tangential direction and a solid line in sagittal direction. In fact, the bandwidth is approximately  $0.015$  (tangential)  $\times 2.2$  (mm) (sagittal), as shown in Fig. 6(a). After the freeform cylindrical lens was introduced, the LSF perfect size was reduced to approximately  $0.015$  (tangential)  $\times 0.015$  (mm) (sagittal), as shown in Fig. 6(b), which is less than  $1/146$  of that in the sagittal direction.

To show the effectiveness of the broadband astigmatism correction, the RMS spot diameter is given as a function to the wavelength for the design with tilting

Table 1. Spectrometer Specifications

Parameter	Value
Central Wavelength (nm)	550
$R_1$ (mm)	100
$R_2$ (mm)	130
$d$ ( $\mu\text{m}$ )	1.67
$\alpha_1$ ( $^\circ$ )	11
$\alpha_2$ ( $^\circ$ )	24.86
$i$ ( $^\circ$ )	9.43
$\bar{\theta}$ ( $^\circ$ )	29.168
$n$	1.5132
$\beta$ ( $^\circ$ )	4.308
$L_{gf}$ (mm)	41.38

Table 2. Spectrometer Initial and Optimized Parameters

Parameter	Calculated	Optimized
$R$ (mm)	2.75	3.389
$t_0$ (mm)	6.30	6.50
$\gamma$ ( $^\circ$ )	26.5967	25.853
$\gamma'$ ( $^\circ$ )	1.467	2.24
$L_{fc}$ (mm)*	52.9585	52.97

\* $L_{fc}$  is the distance between the focusing mirror and the cylindrical lens.

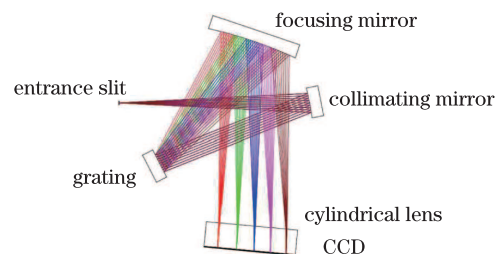


Fig. 4. Layout of the modified Czerny-Turner spectrometer.

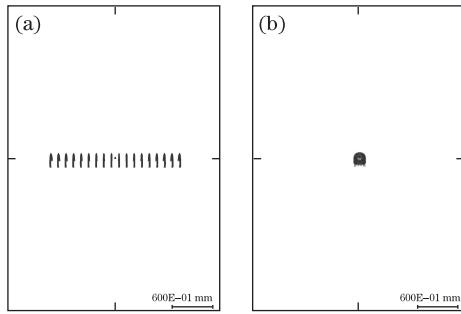


Fig. 5. Spot diagrams of central wavelength for (a) traditional Czerny-Turner spectrometer and (b) freeform cylindrical lens Czerny-Turner spectrometer.

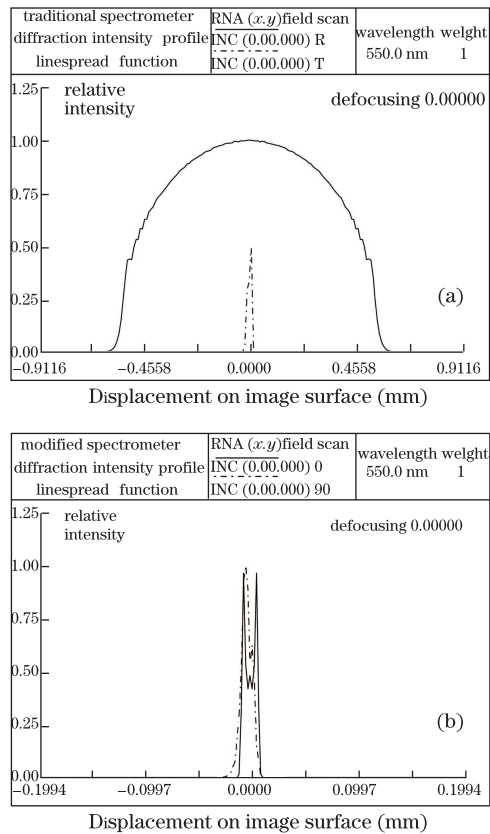


Fig. 6. Line spread function of central wavelength for (a) traditional Czerny-Turner spectrometer and (b) modified Czerny-Turner spectrometer. The dashed rays denote the tangential view, whereas the solid rays denote the sagittal view.

cylindrical lens, a wedge cylindrical lens, and the new design with freeform cylindrical lens. For the same NA, CCD pixel size (i.e.,  $NA=0.05$ , pixel size is  $8 \times 200$  ( $\mu\text{m}$ )) and the same grating with grating period ( $d = 1.67$  ( $\mu\text{m}$ )). From Fig. 7, one can find that the new method has much better performance compared with other methods.

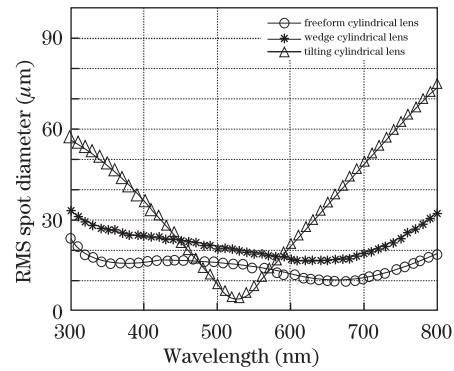


Fig. 7. RMS spot diameters versus wavelength for three different cylindrical lenses: freeform, tilting, and wedge.

In conclusion, using a freeform cylindrical lens, we design a miniature fiber Czerny-Turner spectrometer that can compensate the astigmatism over a broadband spectral range. The design enables practical construction without changing other optical elements, thereby allowing easy modification of the traditional system and greatly improving the spectrometer resolution and the power collection efficiency along the length of the detector system. The resolutions of the spectrometer are 0.4 nm from 300 to 450 nm, 0.3 nm from 450 to 650 nm, and 0.4 nm from 650 to 800 nm. Power collection is enhanced 4.1 times compared with that of the traditional spectrometer. This design will be useful for broad application in miniature broadband spectral measurement.

## References

1. E. Kosik, A. Radunsky, I. Walmsley, and C. Dorrer, *Opt. Lett.* **30**, 326 (2005).
2. R. D. McPeters, S. J. Janz, E. Hilsenrath, T. L. Brown, D. E. Flittner, and D. F. Heath, *Geophys. Res. Lett.* **27**, 2597 (2000).
3. J. P. Rolland, P. Meemon, S. Murali, K. P. Thompson, and K. S. Lee, *Opt. Express* **18**, 3632 (2010).
4. S. Murali, P. Meemon, K. S. Lee, W. P. Kuhn, K. P. Thompson, and J. P. Rolland, *Appl. Opt.* **49**, D145 (2010).
5. A. S. Wyatt, I. A. Walmsley, G. Stibenz, and G. Steinmeyer, *Opt. Lett.* **31**, 1914 (2006).
6. B. Du, L. Li, and Y. Huang, *Chin. Opt. Lett.* **8**, 569 (2010).
7. A. B. Shafer, L. R. Megill, and L. Droppleman, *J. Opt. Soc. Am.* **54**, 879 (1964).
8. Goto and S. Morita, *Rev. Sci. Instrum.* **77**, 10F124 (2006).
9. G. R. Rosendahl, *J. Opt. Soc. Am.* **52**, 412 (1962).
10. M. L. Dalton, Jr., *Appl. Opt.* **5**, 1121 (1966).
11. L. Xu, K. Chen, Q. He, and G. Jin, *Appl. Opt.* **48**, 2871 (2009).
12. D. R. Austin, T. Witting, and I. A. Walmsley, *Appl. Opt.* **48**, 3846 (2009).
13. K. S. Lee, K. P. Thompson, and J. P. Rolland, *Opt. Express* **18**, 23378 (2010).
14. Q. Xue, *Appl. Opt.* **50**, 1338 (2011).
15. H. Li, K. Liu, X. Zhang, T. Zhang, and X. Shen, *Chin. Opt. Lett.* **8**, 329 (2010).